Published in final edited form as:
J Mol Cell Cardiol. 2007 November ; 43(5): 636–647.

Sodium channel *Scn1b* null mice exhibit prolonged QT and RR intervals

Luis F. Lopez-Santiago[1,*], **Laurence S. Meadows**[1,*], **Sara J. Ernst**[4], **Chunling Chen**[1], **Jyoti Dhar Malhotra**[1,3], **Dyke P. McEwen**[1], **Audrey Speelman**[1], **Jeffrey L. Noebels**[4], **Sebastian K.G. Maier**[5], **Anatoli N. Lopatin**[2], and **Lori L. Isom**[1]

1 *Department of Pharmacology, University of Michigan, Ann Arbor, MI 48109*

2 *Department of Molecular & Integrative Physiology, University of Michigan, Ann Arbor, MI 48109*

3 *Department of Biological Chemistry, University of Michigan, Ann Arbor, MI 48109*

4 *Department of Molecular and Human Genetics, Baylor College of Medicine, Houston, Texas 77030*

5 *Medizinische Klinik und Poliklinik I, Universität Würzburg, Würzburg, Germany*

Abstract

In neurons, voltage-gated sodium channel β subunits regulate the expression levels, subcellular localization, and electrophysiological properties of sodium channel α subunits. However, the contribution of β subunits to sodium channel function in heart is poorly understood. We examined the role of β1 in cardiac excitability using *Scn1b* null mice. Compared to wildtype mice, electrocardiograms recorded from *Scn1b* null mice displayed longer RR intervals and extended QT_c intervals, both before and after autonomic block. In acutely dissociated ventricular myocytes, loss of β1 expression resulted in a ~1.6-fold increase in both peak and persistent sodium current while channel gating and kinetics were unaffected. $Na_v1.5$ expression increased in null myocytes ~1.3 fold. Action potential recordings in acutely dissociated ventricular myocytes showed slowed repolarization, supporting the extended QT_c interval. Immunostaining of individual myocytes or ventricular sections revealed no discernable alterations in the localization of sodium channel α or β subunits, $ankyrin_B$, $ankyrin_G$, N-cadherin, or connexin-43. Together, these results suggest that β1 is critical for normal cardiac excitability and loss of β1 may be associated with a long QT phenotype.

Keywords

sodium channel; auxiliary subunit; mouse; ventricular myocyte; cell adhesion; QT-interval

Introduction

Voltage-gated sodium channels play critical roles in both the rising phase and the repolarization phase of the cardiac action potential [1,2]. Mutations in *SCN5A* encoding $Na_v1.5$, the major cardiac channel, result in Long QT and Brugada syndromes [1]. Sodium channels are

Address correspondence to: Lori L. Isom, Ph.D., Department of Pharmacology, University of Michigan, 1301 MSRB III, Ann Arbor, MI 48109-0632, Tel. 734-936-3050, Fax 734-763-4450, lisom@umich.edu..

[*] L.L.S. and L.S.M. contributed equally to this work.

heterotrimers, composed of a single, pore-forming α subunit and two β subunits [3]: a non-covalently linked subunit (β1 or β3) [4,5] and a disulfide-linked subunit (β2 or β4) [6,7]. β subunits are multi-functional molecules that regulate channel cell-surface expression levels and modulate channel function, affecting channel kinetics and voltage-dependence *in vitro* [8]. β subunits also function *in vitro* as homophilic and/or heterophilic cell adhesion molecules that recruit cytoskeletal ankyrin following homophilic cell adhesion [9–11].

While much is known about β1 function *in vitro*, its physiological roles *in vivo* are poorly understood. We showed previously, using *Scn1b* null mice, that β1 plays important roles in the regulation of neuronal excitability *in vivo* [12]. In the present study, we used *Scn1b* null mice to investigate the role of β1 in cardiac excitability. Although the cardiac action potential waveform is significantly different in mice compared to humans, the upstroke, reflecting inward current through sodium channels, as well as the molecular correlates of sodium and potassium channels underlying repolarization, are similar in both species [13]. Thus, gene-targeting strategies in mice can yield valuable insights into the understanding of the role of these channels in human heart and in human disease. Here we examined the cardiac electrophysiology of *Scn1b* null mice. *Scn1b* null cardiomyocytes showed no differences in the voltage-dependence of sodium channel gating or kinetics compared to wildtype littermate mice. In contrast, both I_{Na} and I_{NaP} densities increased approximately 50% in the null mutant. *Scn5a* mRNA and $Na_v1.5$ protein expression increased 51% and 33%, respectively, in the null hearts, consistent with the observed increase in sodium current. Interestingly, [^{3}H]-saxitoxin (STX) binding studies revealed a similar increase in expression levels of tetrodotoxin-sensitive (TTX-S) channels. Surface electrocardiograms (ECGs) showed prolonged QT and RR intervals for *Scn1b* null mice compared to wildtype, which persisted following block of autonomic innervation, suggesting that these effects are due to the absence of β1 in myocytes. Action potential repolarization was prolonged in *Scn1b* null ventricular myocytes, consistent with the prolonged QT phenotype. Localization of sodium channel α and β subunits, as well as localization of structural proteins such as ankyrin, cadherin, and connexin, within myocytes were unaffected by the null mutation. Together, these results demonstrate that β1 is critical for regulation of cardiac electrical excitability. In addition, this represents the first report of a sodium channel-dependent QT prolongation that does not result from altered channel kinetics or voltage-dependence.

MATERIALS AND METHODS

Scn1b null mice

Scn1b null and wildtype mice were generated from *Scn1b* heterozygotes as described [12]. All procedures were performed in accordance with University of Michigan guidelines for animal use and care. The current study was performed on congenic N10–N13 *Scn1b* null, wildtype, and heterozygous male mice on the C57BL/6 background.

Northern blot analysis

Brains and hearts were dissected from anesthetized adult Sprague-Dawley rats, P17-18 *Scn1b* wildtype mice, and P17-18 *Scn1b* null mice. Total RNA was prepared from each sample using Trizol reagent (Invitrogen, Carlsbad, CA), according to the manufacturer's instructions. Northern blots were prepared and probed with a digoxigenin-labeled antisense *Scn1b* probe as previously described [12].

Myocyte isolation

Single ventricular myocytes were extracted from P17-19 *Scn1b* null and wildtype male mice as described [14,15]. Minor modifications included addition of 0.33 mg/ml heparin to the

anesthetic, 50 μM EGTA to solution A, and 25 mg/ml bovine serum albumin to solution C. Only rod-shaped, quiescent cells with smooth striations were selected for examination.

[^{3}H]-STX binding analysis

Ventricular myocytes were isolated from P17 *Scn1b* null or wildtype male mice. [^{3}H]-STX saturation binding analysis was performed on equal aliquots of homogenized cell protein as described [16]. [^{3}H]-STX (28 Ci/mmol) was obtained from Amersham (Piscataway, NJ).

Quantitative RT-PCR

All instruments were sterilized at 200°C for 3–4 hours and treated with RNase Zap (Ambion, Austin, TX) to remove any residual RNases. Littermate sets consisting of *Scn1b* wildtype, heterozygous, and null mice were sacrificed at P14 by decapitation. The hearts were carefully dissected and flash frozen on dry ice/ethanol and stored at −80°C until use. Heart tissue was homogenized using a Tissue-Tearor homogenizer and RNA was isolated using the Qiagen RNeasy Mini Kit (Qiagen, Valencia, CA). RNA was stored at −80°C until use. cDNA was generated from previously collected RNA (1:100 dilution) using Invitrogen (Carlsbad, CA) Super Script III First Strand Synthesis System. The cDNA was then amplified using the Applied Biosystems (ABI, Foster City, CA) 7500 Real Time PCR System and the pre-designed assay available from ABI for mouse *Scn5a* as well as the internal standard *18s* [17]. Fold expression was determined using relative quantification ($2^{-\Delta\Delta Ct}$ method, [18]) normalized to the mean ΔC_t of the wildtypes on each plate and statistics were performed using single factor ANOVA and student's t-tests, $p \leq 0.01$ were considered significant.

Western blot

Heart membrane proteins were isolated using the protocol provided by Alomone Labs (Jerusalem, Israel) and total protein content was quantified using the Bradford assay. 30 μg of heart membrane protein were loaded per lane, separated by 4–20% SDS-PAGE gradient gel, transferred electrophoretically to PVDF-Plus Transfer Membranes, and blotted as described previously [19]. The *Scn5a* antibody was obtained from Alomone Labs and used at 1:200 dilution. The HRP-conjugated secondary goat anti-rabbit antibody was obtained from Santa Cruz Biotechnology, Inc. (Santa Cruz, CA, antibody # SC-2004) and used at 1:5000 dilution. Antibody detection was performed using Amersham (Piscataway, NJ) ECL Western Blotting Analysis System. Bands were quantified using SynGene (Frederick, MD) Gene Tools gel quantification system, corrected for background, and a paired t-test was performed using the one-tailed p-value to determine significance.

Antibodies

Antibodies were obtained from the following sources: anti-$Na_v1.5$ (for immunocytochemistry), anti-β3, and anti-β4: Dr. W.A. Catterall, University of Washington [9,20,21]; anti-*Scn5a* (ASC-005, for Western blotting): Alomone Labs (Jerusalem, Israel); anti-$Na_v1.1$ (K74/71) and anti-$Na_v1.6$ (K87A/10): UC Davis/NINDS/NIMH Neuromab Facility; anti-$Na_v1.4$: Dr. S. Kraner, University of Kentucky [22]; anti-connexin-43: Chemicon (Temecula, CA); anti-α-actinin: Sigma-Aldrich (St. Louis, MO); anti-N-cadherin: Santa Cruz Biotechnology Inc. (Santa Cruz, CA); Alexa-fluor (546 nm)-conjugated phalloidin and Alexa-fluor secondary antibody conjugates (488 nM and 544 nM): Molecular Probes (Eugene, OR); anti-$ankyrin_B$: Zymed Laboratories Inc. (South San Francisco, CA); anti-$ankyrin_G$: Dr. V. Bennett, Duke University [23]. Anti-$\beta1_{ex}$ was described previously [12].

Immunochemistry

P17 male mice were anesthetized and perfused and isolated hearts or individual myocytes were prepared for immunocytochemistry as described [11]. Anti-$Na_v1.5$, anti-β3, anti-β4, anti-

$Na_v1.6$, anti-$\beta1_{ex}$, anti-connexin-43, and anti-$ankyrin_B$ were applied at 1:100 dilution; anti-N-cadherin at 1:50; anti-$Na_v1.1$ at 1:50; anti-α-actinin at 1:200; Alexa-fluor (546 nm)-conjugated phalloidin diluted 1:100. Secondary antibodies (Alexa-flour conjugates) were diluted 1:200. Sections were visualized with an Olympus (Center Valley, PA) FluoView 500 confocal laser scanning microscope in the Microscopy and Image Analysis Laboratory Core Facility (MIAL) at the University of Michigan.

Measurement of I_{Na}

Voltage-clamp recordings were performed at room temperature in the whole cell configuration using an Axopatch 200B amplifier and pClamp (versions 8.2 and 9.2, Axon Instruments, Foster City, CA) with 1.5–2.5 MΩ patch pipettes. Solutions were prepared as described [20], including 5 mM extracellular NaCl adjusted to pH 7.4 with CsOH. Series resistance was compensated 40–65% and leak subtraction performed by application of a standard P/4 protocol. Holding potential was −100 mV. Activation curves were determined via application of 190 ms pulses from −80 to +35 mV in 5 mV increments. Inactivation curves were generated via application of a 100 ms conditioning pulse from −120 to 0 mV in 5 mV increments followed by a 7.5 ms test pulse to 0 mV. Normalized conductance and inactivation curves were generated as described previously [16]. τ_{fast} and τ_{slow} were determined by fitting the decay phase of currents with the sum of two exponentials. To determine τ_{rec}, Na_v1s were inactivated with a 5 ms pulse to 0 mV, followed by a recovery pulse of variable duration to −100 mV, a subsequent test pulse to 0 mV to determine the fraction of recovered channels, and the resultant data fit with a single exponential. I_{NaP} amplitude was calculated from the average current amplitude 50–100 ms after the start of the test pulse. Current densities were determined by dividing current amplitude by the cell capacitance (C_m), as determined by application of +10 mV depolarizing test pulses.

Action potential measurements

Acutely isolated left ventricular myocytes were bathed at room temperature in 1x HBSS supplemented with 20 mM HEPES, pH 7.3. Patch pipettes (1.0–3.0 MΩ) were filled with (in mM): 135 KCl, 10 NaCl, 1 $CaCl_2$, 10 EGTA and 10 HEPES, pH 7.4 with KOH. The resting potential (Rp) was determined under current clamp at zero current. The stimulus to elicit an action potential (threshold current) was determined by application of 3 ms test pulses every 2.5 s, starting at 0.2 nA and increasing by 0.05 nA until an action potential was observed. Subsequent action potentials were evoked by application of 12 × 3 ms test pulses at 1.5x threshold. Myocytes were paced at cycle lengths (CLs) of 150, 300, or 1000 ms, data filtered at 5 kHz and sampled at 20 kHz. Action potential amplitudes were measured from Rp to the peak. Action potential durations (APDs) were measured from the start of the stimulatory pulse to 25, 50, 75, and 90% decay of the peak to Rp (APD_{25}, APD_{50}, APD_{75}, or APD_{90}, respectively). Finally, the maximum rates of depolarization and repolarization were measured from the differentiated waveform. Comparison of APDs between wild type and *Scn1b* null myocytes was carried out using two-way ANOVA (GraphPad Prism 3.0, GraphPad Software Inc., USA.

ECG recording

Standard 3-lead surface ECGs of P17 *Scn1b* null, heterozygous, and wildtype male mice were recorded as described [15]. Acquisition was performed 8–10 min following anesthesia and data collected for 8 consecutive min at a sampling rate of 5 kHz using a DP304 differential amplifier (Warner Instruments Corp., Hamden, CT). To examine the effects of autonomic block on the ECG, each mouse was subsequently injected (10 μl/g i.p.) with propranolol and atropine (20 mg/kg and 1 mg/kg, respectively) in 0.9% saline. ECGs were then immediately recorded for 15 uninterrupted min. Lead 2 data were analyzed by two independent investigators using two different approaches. The first investigator (Investigator 1) calculated parameters for each

individual animal from averages of 20–40 consecutive traces using homemade software (Delphi 5, Borland Int.) [15]. Data were then combined from the averaged measurements for each individual mouse to yield an averaged value for each genotype. QT intervals were calculated for each animal by measuring the interval to the T wave peak (QT_{PEAK}) and to 90% of T wave decay (QT_{90}) to baseline. QT_{PEAK} and QT_{90} values for each mouse represented averaged measurements from 20–40 consecutive traces. QT_{PEAK} and QT_{90} values for each genotype represented averaged values from all mice of the corresponding genotype. To correct for the effect of heart rate on QT_{90} intervals, a heart-rate corrected QT_{90} (QT_{90C}) was generated, as described previously [24]. Briefly, RR and QT_{90} intervals for each mouse (where RR and QT_{90} measurements for each individual mouse each represent the average of measurements from 20–40 consecutive traces) were plotted in the form of (ln(RR/100) vs. ln (QT_{90}). The resultant data from all mice of a given genotype were then subjected to a linear fit where QT_{90c} was calculated as the intercept of the linear fit of the data with the y axis. To confirm the results of the first analysis, a second investigator (Investigator 2) analyzed a minimum of 150 individual cycles within an observation period of 2 min, using EMKA-software (Emka Technologies, Paris, France). The value of each ECG parameter of each single cycle was assessed and data averaged.

RESULTS

Molecular characterization of Scn1b null mice

We showed previously that *Scn1b* null mice lack *Scn1b* mRNA in brain [12]. Fig. 1 demonstrates the complete absence of *Scn1b* mRNA in heart as well as brain in these mice. Consistent with previous work [25], mice have lower levels of *Scn1b* mRNA in heart compared to brain, and this difference in transcript levels is species-specific, as levels of *Scn1b* mRNA in rat brain and rat heart are similar.

Loss of β1 does not alter sodium channel voltage-dependence or kinetics

Consistent with previous studies of *Scn1b* null hippocampal and cerebellar Purkinje neurons [12,26], no significant differences were detected in the voltage-dependence of sodium channel activation or inactivation (Fig. 2B), time-course of inactivation (Fig. 2C,Table 1), or recovery from inactivation (Fig. 2D) in *Scn1b* null myocytes. In contrast, a ~1.6-fold increase in both I_{Na} (Fig. 2A and 3A) and I_{NaP} (Fig. 3B) densities was observed for myocytes from null mice compared to wildtype. While we were not able to measure consistent differences in the TTX-S component of I_{Na} due to technical issues with current stability over long experiments, [^{3}H]-STX binding revealed a proportionally similar increase (~1.9-fold) in homogenates of ventricular myocytes, suggesting that at least a portion of this effect may be attributable to increased TTX-S channel expression (Fig. 3C). It has been shown previously that the proportion of TTX-S I_{Na} in mouse ventricular myocytes is very small and detectable only after activation with β-scorpion toxin [20], likely explaining our inability to reliably measure these currents.

Increased Scn5a mRNA and $Na_v1.5$ in Scn1b null heart tissue

Quantitative RT-PCR in 6 P14 littermate sets (*Scn1b* wildtype, heterozygous, and null mice) revealed no significant change in *Scn5a* mRNA expression in heterozygous hearts compared to wildtype. However, a significant increase in *Scn5a* mRNA expression was observed in *Scn1b* null hearts compared to wildtype (~1.5 fold, $p = 0.002$) (Fig. 3D, upper panel). Western blot analysis of heart membrane protein isolated from 3 P14 littermate pairs revealed an increase in $Na_v1.5$ protein in *Scn1b* null hearts relative to wildtype that was similar to the observed increases in I_{Na} and I_{NaP} (~1.3 fold, $p = 0.03$) (Fig. 3D, lower panel). Protein size, as well as splicing assay (RT-PCR) data (not shown), were consistent with the full length, functional splice form of *Scn5a* previously identified [27]. In similar Western blot experiments,

we observed no differences in the expression levels of β2, β3, or β4 in *Scn1b* null hearts compared to wildtype, indicating that these other sodium channel β subunit proteins did not compensate for the loss of β1 (data not shown).

Surface ECG recordings

ECGs of anesthetized P17-18 male mice were examined. QT intervals were measured to the T wave peak (QT_{PEAK}) and to 90% of T decay (QT_{90}). *Scn1b* null mice displayed ECGs with prolonged QT_{PEAK} (by ~3 ms, $p \leq 0.001$) and QT_{90} intervals (by ~5 ms, $p \leq 0.001$, Table 2) compared to wildtype mice. The RR interval for *Scn1b* null mice was also longer (by ~20 ms, $p = 0.02$), indicating a slower heart rate. ECG parameters of *Scn1b* heterozygous mice were statistically indistinguishable from those of wildtype. Since the longer QT_{90} interval of *Scn1b* null mice could reflect alterations in heart rate, a heart-rate corrected QT_{90} (QT_{90C}) was generated as described [24] (Table 2). As with QT_{90}, QT_{90C} intervals were longer (~1.5-fold) in null mice, indicating that differences in heart rate were not responsible for the prolonged QT interval. No significant differences were observed in other ECG parameters between *Scn1b* null and wildtype mice.

In view of the neurological effects resulting from the loss of β1 expression [12], it was possible that the altered ECG waveform of *Scn1b* null mice resulted from impaired cardiac innervation. To examine this, ECGs were recorded following administration of propranolol and atropine to block β-adrenergic and muscarinic receptors, respectively [28]. Following autonomic block, the R wave amplitude and P, QRS, and PR durations remained similar between mice of all three genotypes (Table 2), although compared to control recordings the administration of propranolol and atropine resulted in longer P (by ~1 ms) and QRS (~ 0.5–2 ms) components (Table 2). Compared to control recordings, $QT_{Peak,}$ was also lengthened (~3 ms) but not QT_{90} however, following autonomic block both QT intervals remained longer for $\beta1^{-/-}$ mice compared to those of wildtype and heterozygous animals. The RR interval for *Scn1b* null mice was also longer than control animals and remained significantly longer than those of wildtype and heterozygous mice following block. Furthermore, the difference in QT_{90C} for *Scn1b* null mice compared to wildtype or heterozygous animals (>10 ms longer under control conditions) was even more pronounced following autonomic block (>20 ms longer).

Loss of β1 results in prolongation of action potential repolarization

Action potentials were compared between *Scn1b* null and wildtype left ventricular myocytes. No differences were observed in resting membrane potentials (*Scn1b* null: −80.1 ± 0.9 mV vs. *Scn1b* wildtype: −80.5 ± 0.5 mV, n =15 for each genotype, $p = 0.77$), or in the current necessary to elicit an action potential (*Scn1b* null: 0.53 ± 0.04 nA vs. *Scn1b* wildtype: 0.62 ± 0.04 nA, n = 15 for each genotype, $p = 0.15$). To mimic physiological heart rates, stimulus pulses were initially applied every 100 ms. Under these conditions, and for both genotypes, action potentials exhibited dramatic lengthening in duration such that it was not possible to measure APDs of later action potentials (not shown). We found, however, that the use of longer CLs made this analysis possible, as demonstrated below.

Action potentials were elicited by applying test pulses every 150 ms (6.7 Hz), intervals similar to the average RR intervals of anesthetized wildtype mice (Table 2). Repeated stimulation resulted in AP lengthening for successive action potentials for both genotypes, but APs were significantly longer in *Scn1b* null myocytes (Fig. 4). In particular, in *Scn1b* null cells APD_{75} was ~ 20 ms larger at any given AP number ($p < 0.0001$ using two-way ANOVA). APD_{25}, APD_{50} and APD_{90} were also significantly prolonged in *Scn1b* null cells ($p < 0.05$, data not shown). In contrast, action potential amplitudes were similar between both sets of myocytes: *Scn1b* wildtype: 128.9 ± 1.9, *Scn1b* null: 128.5 ± 0.9 mV (p=0.84).

We next analyzed the rate of change in membrane potential (V_m), calculated as the first derivative of V_m, dV_m/dt (Fig. 5A). We observed a small but significant 13% reduction in the time required to reach the maximum rate of depolarization in the null myocytes. *Scn1b* null myocytes reached the maximum rate of depolarization rate earlier than *Scn1b* wildtype cells ($p=0.0021$ for CL150, Fig. 5B). We also observed a 25–30% reduction in the maximum rate of repolarization in *Scn1b* null myocytes compared to wildtype for CL150 and CL300 (Fig. 5C, $p < 0.05$). (Differences observed for CL1000 were not significant and are not shown). We propose that the observed increase in I_{NaP} recorded in *Scn1b* null myocytes is responsible for this prolongation of ventricular repolarization.

Localization of sodium channel α and β subunits

Sodium channel expression is altered in *Scn1b* null hippocampus [12]. Thus, we predicted that loss of β1 in heart might similarly perturb sodium channel expression. To test our hypothesis, we examined the localization of sodium channel subunits in acutely dissociated cardiomyocytes and in ventricular slices obtained from *Scn1b* null and *Scn1b* wildtype mice. In ventricular sections obtained from male *Scn1b* null and wildtype mice, α-actinin (Fig. 6A, 6B), $ankyrin_B$ (Fig. 7A), and phalloidin (Fig. 6E, 6F) localized to the Z-line/t-tubules while $ankyrin_G$ (Fig. 7B), N-cadherin (Fig. 7C), and connexin-43 (Fig. 7C,6I, 6J) were localized to the intercalated disks, consistent with previous studies [11,23,29]. We found similar results in studies on acutely dissociated ventricular myocytes performed in parallel (not shown).

In ventricular sections (Fig. 6) and in acutely dissociated myocytes (not shown) obtained from both genotypes, $Na_v1.1$ (Fig. 6A, 6B) and $Na_v1.6$ (Fig. 6E, 6F) were detected at Z-lines/t-tubules, consistent with previous reports [20,29]. Prominent clustering of $Na_v1.5$ was detected at intercalated disks as well as at the cell surface (Fig. 6C, 6D), consistent with previous observations [20,21,29,30]. No changes in $Na_v1.5$ localization were observed in spite of increased protein expression (Fig. 3). We also examined the localization of β3 and β4 (sufficient anti-β2 was not available for this study). In agreement with previous reports, β3 (Fig. 6G, 6H) and β4 (Fig. 6I, 6J) remained localized at Z-lines/t-tubules and intercalated disks, respectively [21].

Body to heart weight ratio

Scn1b null mice are smaller than age-matched, wildtype littermates, with an average body weight at P17 of 4.79 ± 0.06 g (n = 48) vs. 6.51 ± 0.18 g for *Scn1b* wildtype mice (n = 34, $p < 0.001$). We compared the relative ratios of total body weight to heart weight for our two sets of animals. *Scn1b* wildtype mice showed an average heart weight of 48.3 ± 1.6 mg, with a resultant average ratio of 136 ± 2.3. In contrast, *Scn1b* null mice displayed an average heart weight of 32.8 ± 0.8 mg ($p < 0.001$) and an average ratio of 147 ± 2.7 ($p < 0.003$), suggesting that the *Scn1b* null mutation may affect heart development, possibly through modulation of electrical excitability and/or through modulation of cell adhesion.

DISCUSSION

To investigate the role of sodium channel β1 subunits in cardiac electrophysiology, surface ECGs, whole cell I_{Na}, action potentials, RT-PCR, Western blot analyses, [^{3}H]-STX binding, and channel subunit subcellular localization were compared between *Scn1b* null and wildtype mice. Although channel kinetics and voltage-dependence were unaffected, loss of β1 resulted in increases in both I_{Na} and I_{NaP} densities that were supported by similar increases in $Na_v1.5$ expression and [^{3}H]-STX binding. ECGs of *Scn1b* null mice showed significantly lengthened QT and RR intervals that remained following block of autonomic innervation. Action potential duration was significantly longer in *Scn1b* null ventricular myocytes and the rate of action potential repolarization was significantly slowed in *Scn1b* null ventricular myocytes compared

to wildtype, consistent with the prolonged QT interval. We propose that increases in I_{NaP} underlie in part the observed changes in action potential repolarization in *Scn1b* null myocytes and that the combination of increased depolarizing I_{Na} and increased I_{NaP} are responsible in part for QT prolongation [1], although it is possible that the *Scn1b* null mutation also affects potassium currents, as discussed below. This is the first report of a long QT phenotype involving sodium channels that does not appear to result from changes in $Na_v1.5$ kinetics or voltage-dependence. Alternatively, or in addition, potassium current may play a functional role, as changes in potassium channel availability can dramatically alter the cardiac action potential [31]. Intriguingly, studies using heterologous expression systems have suggested that β1 may associate with and modulate, $K_v4.3$, which contributes to transient outward current (I_{to}) in human and mouse ventricle [32,33]. This interesting possibility will be the focus of future studies.

Coexpression of β1 with TTX-S sodium channel α subunits in heterologous systems *in vitro* results in increased I_{Na}, increased rates of channel activation and inactivation, and shifts in the voltage-dependence of activation and inactivation [4,34]. Interestingly, results from acutely isolated *Scn1b* null hippocampal and cerebellar neurons, which express primarily TTX-S channels, showed none of these effects [12,26], suggesting that the physiological roles of β1 may be cell type specific and, importantly, that heterologous expression systems cannot mimic the situation in neurons. Previous studies describing the effects of β1 on TTX-R $Na_v1.5$ *in vitro* have yielded variable results, depending on the heterologous expression system utilized. In contrast to TTX-S channels, expression of $Na_v1.5$ in oocytes generates I_{Na} that inactivates rapidly in the absence of β subunits [35]. According to some reports, β1 has no observable effect on $Na_v1.5$ function [36,37]. Other groups have reported that coexpression of β1 and $Na_v1.5$ results in increased I_{Na} density with no detectable effects on gating [35,38]. Some groups have reported modulation of channel sensitivity to lidocaine block with subtle changes in gating properties in response to β1 expression [39], while others have reported significant shifts in the voltage-dependence of steady-state inactivation [29,40] or the rate of recovery from inactivation [41]. The most interesting result of heterologous expression studies in terms of the present data is the finding that β1 coexpression decreases I_{NaP} in HEK cells [42], implying that the loss of β1 expression increases I_{NaP}, consistent with our *in vivo* results. While HEK cells do not accurately mimic the situation in cardiac myocytes, it is interesting to consider the suggestion from these authors that down-regulation of β1 or disruption of α-β1 interactions might contribute to a prolonged QT phenotype. Indeed, the *SCN5A* D1790G long QT mutation disrupts the ability of $Na_v1.5$ to be modulated by β1 [40]. Cytoskeletal disruption in cardiac myocytes induces sodium channels to exhibit increased I_{NaP} [43]. This is also consistent with deletion of β1, a cell adhesion molecule that links sodium channels to the cytoskeleton via ankyrin [9].

Scn1b null mice exhibit significantly prolonged RR intervals in addition to prolonged QT intervals. A group of *SCN5A* mutations that give rise to I_{NaP} not only underlie QT-prolongation, but also result in sinus bradycardia and sinus pauses and have been postulated to be a direct cause of sudden death in some patients [44,45]. This group of mutations includes the LQT3 mutant, D1790G, which interrupts sodium channel α-β1 interactions [40]. Mutations in ankyrin-B cause a dominantly-associated cardiac syndrome that includes sick sinus syndrome, bradycardia, and risk of sudden cardiac death [46]. This syndrome, originally classified as LQT4, was later renamed, as prolonged QT intervals are not consistent features. Although as yet uninvestigated, it is likely that β1 subunits are expressed in sinoatrial node as well as in ventricle where they may regulate heart rate through I_{NaP} and channel-cytoskeletal interactions.

Multiple TTX-S sodium channels are expressed in heart [20,29,47]. Several lines of evidence have shown that TTX-S channels are localized at t-tubules in ventricular myocytes [21,29] and in sinoatrial node [47,48], although the physiological role of these channels is not well

understood [20,49]. We propose that at least a portion of the increased I_{NaP} observed in *Scn1b* null myocytes may be attributable to one or more TTX-S channels in addition to effects on TTX-R $Na_v1.5$. This conclusion, which is supported by our [^{3}H]-STX binding data, must be tempered by our inability to measure reliable differences in TTX-S I_{Na} in *Scn1b* null myocytes due to technical limitations. Nanomolar concentrations of TTX shorten the mammalian cardiac action potential, as first demonstrated by [50], suggesting that TTX-S channels can generate I_{NaP}. Until the contributions of TTX-S currents to the total I_{Na} in mouse ventricular myocytes can be resolved, however, the involvement of TTX-S sodium channels in increased I_{NaP} in *Scn1b* null myocytes remains unknown. Nevertheless, it is interesting to consider that the effects of β1 *in vivo* are cell type specific and may even be subcellular domain specific. Our results, combined with our previous report on *Scn1b* null mice [12], emphasize the importance of studying ion channels in their native environment.

Acknowledgements

This work was supported by AHA Established Investigator Award 0140133N to LLI, by R01MH059980 to LLI, by R01HL69052 to ANL, by R01NS29709 to JLN, and by the Deutsche Forschungsgemeinschaft to SKGM (Ma 2252). The authors gratefully acknowledge Dr. Penelope Boyden, Dr. Jeanne Nerbonne and Dr. William Brackenbury for many helpful discussions and Meredith McLerie, Emily Slat, and Travis Dickendesher for expert technical assistance.

References

1. Tan HL, Bezzina CR, Smits JP, Verkerk AO, Wilde AA. Genetic control of sodium channel function. Cardiovasc Res 2003 Mar 15;57(4):961–73. [PubMed: 12650874]
2. Meadows LS, Isom LL. Sodium channels as macromolecular complexes: implications for inherited arrhythmia syndromes. Cardiovascular Research 2005;67:448–58. [PubMed: 15919069]
3. Hartshorne RP, Messner DJ, Coppersmith JC, Catterall WA. The saxitoxin receptor of the sodium channel from rat brain Evidence for two nonidentical beta subunits. JBiolChem 1982;257:13888–91.
4. Isom LL, De Jongh KS, Patton DE, Reber BFX, Offord J, Charbonneau H, et al. Primary structure and functional expression of the β1 subunit of the rat brain sodium channel. Science 1992;256:839–42. [PubMed: 1375395]
5. Morgan K, Stevens EB, Shah B, Cox PJ, Dixon AK, Lee K, et al. β3: An additional auxiliary subunit of the voltage-sensitive sodium channel that modulates channel gating with distinct kinetics. Proc Natl Acad Sci USA 2000;97:2308–13. [PubMed: 10688874]
6. Isom LL, Ragsdale DS, De Jongh KS, Westenbroek RE, Reber BF, Scheuer T, et al. Structure and function of the β2 subunit of brain sodium channels, a transmembrane glycoprotein with a CAM motif. Cell 1995;83:433–42. [PubMed: 8521473]
7. Yu FH, Westenbroek RE, Silos-Santiago I, McCormick KA, Lawson D, Ge P, et al. Sodium channel beta4, a new disulfide-linked auxiliary subunit with similarity to beta2. J Neurosci 2003 Aug 20;23 (20):7577–85. [PubMed: 12930796]
8. Isom LL. Sodium channel β subunits: anything but auxiliary. The Neuroscientist 2001;7:42–54. [PubMed: 11486343]
9. Malhotra JD, Kazen-Gillespie K, Hortsch M, Isom LL. Sodium channel β subunits mediate homophilic cell adhesion and recruit ankyrin to points of cell-cell contact. J Biol Chem 2000;275:11383–8. [PubMed: 10753953]
10. Malhotra JD, Koopmann MC, Kazen-Gillespie KA, Fettman N, Hortsch M, Isom LL. Structural requirements for interaction of sodium channel β1 subunits with ankyrin. J Biol Chem 2002;277(29): 26681–8. [PubMed: 11997395]
11. Malhotra JD, Thyagarajan V, Chen C, Isom LL. Tyrosine-phosphorylated and nonphosphorylated sodium channel beta1 subunits are differentially localized in cardiac myocytes. J Biol Chem 2004 Sep 24;279(39):40748–54. [PubMed: 15272007]
12. Chen C, Westenbroek RE, Xu X, Edwards CA, Sorenson DR, Chen Y, et al. Mice lacking sodium channel beta1 subunits display defects in neuronal excitability, sodium channel expression, and nodal architecture. J Neurosci 2004 Apr 21;24(16):4030–42. [PubMed: 15102918]

13. Nerbonne JM. Studying cardiac arrhythmias in the mouse--a reasonable model for probing mechanisms? Trends Cardiovasc Med 2004 Apr;14(3):83–93. [PubMed: 15121155]
14. Lopatin AN, Shantz LM, Mackintosh CA, Nichols CG, Pegg AE. Modulation of potassium channels in the hearts of transgenic and mutant mice with altered polyamine biosynthesis. J Mol Cell Cardiol 2000 Nov;32(11):2007–24. [PubMed: 11040105]
15. McLerie M, Lopatin AN. Dominant-negative suppression of I(K1) in the mouse heart leads to altered cardiac excitability. J Mol Cell Cardiol 2003 Apr;35(4):367–78. [PubMed: 12689816]
16. Meadows L, Malhotra JD, Stetzer A, Isom LL, Ragsdale DS. The intracellular segment of the sodium channel β1 subunit is required for its efficient association with the channel α subunit. J Neurochem 2001;76:1871–8. [PubMed: 11259505]
17. Burbach GJ, Dehn D, Nagel B, Del Turco D, Deller T. Laser microdissection of immunolabeled astrocytes allows quantification of astrocytic gene expression. J Neurosci Methods 2004 Sep 30;138 (1–2):141–8. [PubMed: 15325122]
18. Livak KJ, Schmittgen TD. Analysis of relative gene expression data using real-time quantitative PCR and the 2(−Delta Delta C(T)) Method. Methods 2001 Dec;25(4):402–8. [PubMed: 11846609]
19. Zicha S, Maltsev VA, Nattel S, Sabbah HN, Undrovinas AI. Post-transcriptional alterations in the expression of cardiac Na+ channel subunits in chronic heart failure. J Mol Cell Cardiol 2004 Jul;37 (1):91–100. [PubMed: 15242739]
20. Maier SK, Westenbroek RE, Schenkman KA, Feigl EO, Scheuer T, Catterall WA. An unexpected role for brain-type sodium channels in coupling of cell surface depolarization to contraction in the heart. Proc Natl Acad Sci U S A 2002 Mar 19;99(6):4073–8. [PubMed: 11891345]
21. Maier SK, Westenbroek RE, McCormick KA, Curtis R, Scheuer T, Catterall WA. Distinct subcellular localization of different sodium channel alpha and beta subunits in single ventricular myocytes from mouse heart. Circulation 2004 Mar 23;109(11):1421–7. [PubMed: 15007009]
22. Thompson AL, Filatov G, Chen C, Porter I, Li Y, Rich MM, et al. A selective role for MRF4 in innervated adult skeletal muscle: Na(V) 1.4 Na+ channel expression is reduced in MRF4-null mice. Gene Expr 2005;12(4–6):289–303. [PubMed: 16358417]
23. Mohler PJ, Rivolta I, Napolitano C, LeMaillet G, Lambert S, Priori SG, et al. Nav1.5 E1053K mutation causing Brugada syndrome blocks binding to ankyrin-G and expression of Nav1.5 on the surface of cardiomyocytes. Proc Natl Acad Sci U S A 2004 Dec 14;101(50):17533–8. [PubMed: 15579534]
24. Mitchell GF, Jeron A, Koren G. Measurement of heart rate and Q-T interval in the conscious mouse. Am J Physiol 1998 Mar;274(3 Pt 2):H747–51. [PubMed: 9530184]
25. Grosson CL, Cannon SC, Corey DP, Gusella JF. Sequence of the voltage-gated sodium channel beta1-subunit in wild-type and in quivering mice. Brain Res Mol Brain Res 1996;42(2):222–6. [PubMed: 9013777]
26. Grieco TM, Malhotra JD, Chen C, Isom LL, Raman IM. Open-channel block by the cytoplasmic tail of sodium channel β4 as a mechanism for resurgent sodium current. Neuron 2005;45:233–44. [PubMed: 15664175]
27. Zimmer T, Bollensdorff C, Haufe V, Birch-Hirschfeld E, Benndorf K. Mouse heart Na+ channels: primary structure and function of two isoforms and alternatively spliced variants. Am J Physiol Heart Circ Physiol 2002 Mar;282(3):H1007–17. [PubMed: 11834499]
28. Zhang Z, Xu Y, Song H, Rodriguez J, Tuteja D, Namkung Y, et al. Functional Roles of Ca(v)1.3 (alpha(1D)) calcium channel in sinoatrial nodes: insight gained using gene-targeted null mutant mice. Circ Res 2002 May 17;90(9):981–7. [PubMed: 12016264]
29. Malhotra JD, Chen C, Rivolta I, Abriel H, Malhotra R, Mattei LN, et al. Characterization of Sodium Channel α and β subunits in Rat and Mouse Cardiac Myocytes. Circulation 2001;103:1303–10. [PubMed: 11238277]
30. Cohen SA. Immunocytochemical localization of rH1 sodium channel in adult rat heart atria and ventricle. Presence in terminal intercalated disks. Circulation 1996;94(1):3083–6. [PubMed: 8989112]
31. Ishihara K, Yan DH, Yamamoto S, Ehara T. Inward rectifier K(+) current under physiological cytoplasmic conditions in guinea-pig cardiac ventricular cells. J Physiol 2002 May 1;540(Pt 3):831–41. [PubMed: 11986372]

32. Deschenes I, Tomaselli GF. Modulation of Kv4.3 current by accessory subunits. FEBS letters 2002 Sep 25;528(1–3):183–8. [PubMed: 12297301]
33. Nerbonne JM, Kass RS. Molecular physiology of cardiac repolarization. Physiol Rev 2005 Oct;85 (4):1205–53. [PubMed: 16183911]
34. Isom LL, Scheuer T, Brownstein AB, Ragsdale DS, Murphy BJ, Catterall WA. Functional co-expression of the β1 and type IIA α subunits of sodium channels in a mammalian cell line. J Biol Chem 1995;270:3306–12. [PubMed: 7852416]
35. Qu Y, Isom LL, Westenbroek RE, Rogers JC, Tanada TN, McCormick KA, et al. Modulation of cardiac Na+ channel expression in Xenopus oocytes by β1 subunits. J Biol Chem 1995;270:25696–701. [PubMed: 7592748]
36. Makita N, Bennett PB Jr, George AL Jr. Voltage-gated Na^+ channel β1 subunit mRNA expressed in adult human skeletal muscle, heart, and brain is encoded by a single gene. J Biol Chem 1994;269:7571–8. [PubMed: 8125980]
37. Yang JS, Bennett PB, Makita N, George AL, Barchi RL. Expression of the sodium channel β1 subunit in rat skeletal muscle is selectively associated with the tetrodotoxin-sensitive α subunit isoform. Neuron 1993;11:915–22. [PubMed: 8240813]
38. Nuss HB, Chiamvimonvat N, Perez-Garcia MT, Tomaselli GF, Marban E. Functional association of the beta 1 subunit with human cardiac (hH1) and rat skeletal muscle (μ1) sodium channel alpha subunits expressed in Xenopus oocytes. J Gen Physiol 1995;106:1171–91. [PubMed: 8786355]
39. Makielski JC, Limberis JT, Chang SY, Fan Z, Kyle JW. Coexpression of beta 1 with cardiac sodium channel alpha subunits in oocytes decreases lidocaine block. Mol Pharmacol 1996;49(1):30–9. [PubMed: 8569709]
40. An RH, Wang XL, Kerem B, Benhorin J, Medina A, Goldmit M, et al. Novel LQT-3 mutation affects Na^+ channel activity through interactions between alpha- and beta1-subunits. Circ Res 1998;83:141–6. [PubMed: 9686753]
41. Fahmi AI, Patel M, Stevens EB, Fowden AL, John JE 3rd, Lee K, et al. The sodium channel beta-subunit SCN3b modulates the kinetics of SCN5a and is expressed heterogeneously in sheep heart. J Physiol 2001 Dec 15;537(Pt 3):693–700. [PubMed: 11744748]
42. Valdivia CR, Nagatomo T, Makielski JC. Late Na currents affected by alpha subunit isoform and beta1 subunit co-expression in HEK293 cells. J Mol Cell Cardiol 2002 Aug;34(8):1029–39. [PubMed: 12234772]
43. Undrovinas AI, Shander GS, Makielski JC. Cytoskeleton modulates gating of voltage-dependent sodium channel in heart. Am J Physiol 1995;269:H203–14. [PubMed: 7631850]
44. Schwartz PJ, Priori SG, Spazzolini C, Moss AJ, Vincent GM, Napolitano C, et al. Genotype-phenotype correlation in the long-QT syndrome: gene-specific triggers for life-threatening arrhythmias. Circulation 2001 Jan 2;103(1):89–95. [PubMed: 11136691]
45. Veldkamp MW, Wilders R, Baartscheer A, Zegers JG, Bezzina CR, Wilde AA. Contribution of sodium channel mutations to bradycardia and sinus node dysfunction in LQT3 families. Circ Res 2003 May 16;92(9):976–83. [PubMed: 12676817]
46. Mohler PJ, Bennett V. Ankyrin-based cardiac arrhythmias: a new class of channelopathies due to loss of cellular targeting. Curr Opin Cardiol 2005 May;20(3):189–93. [PubMed: 15861006]
47. Maier SK, Westenbroek RE, Yamanushi TT, Dobrzynski H, Boyett MR, Catterall WA, et al. An unexpected requirement for brain-type sodium channels for control of heart rate in the mouse sinoatrial node. Proc Natl Acad Sci U S A 2003 Mar 18;100(6):3507–12. [PubMed: 12631690]
48. Lei M, Jones SA, Liu J, Lancaster MK, Fung SS, Dobrzynski H, et al. Requirement of neuronal- and cardiac-type sodium channels for murine sinoatrial node pacemaking. J Physiol 2004 Sep 15;559(Pt 3):835–48. [PubMed: 15254155]
49. Brette F, Orchard CH. No apparent requirement for neuronal sodium channels in excitation-contraction coupling in rat ventricular myocytes. Circ Res 2006 Mar 17;98(5):667–74. [PubMed: 16484618]
50. Dudel J, Peper K, Rudel R, Trautwein W. Effect of tetrodotoxin on membrane currents in mammalian cardiac fibres. Nature 1967 Jan 21;213(73):296–7. [PubMed: 6030617]

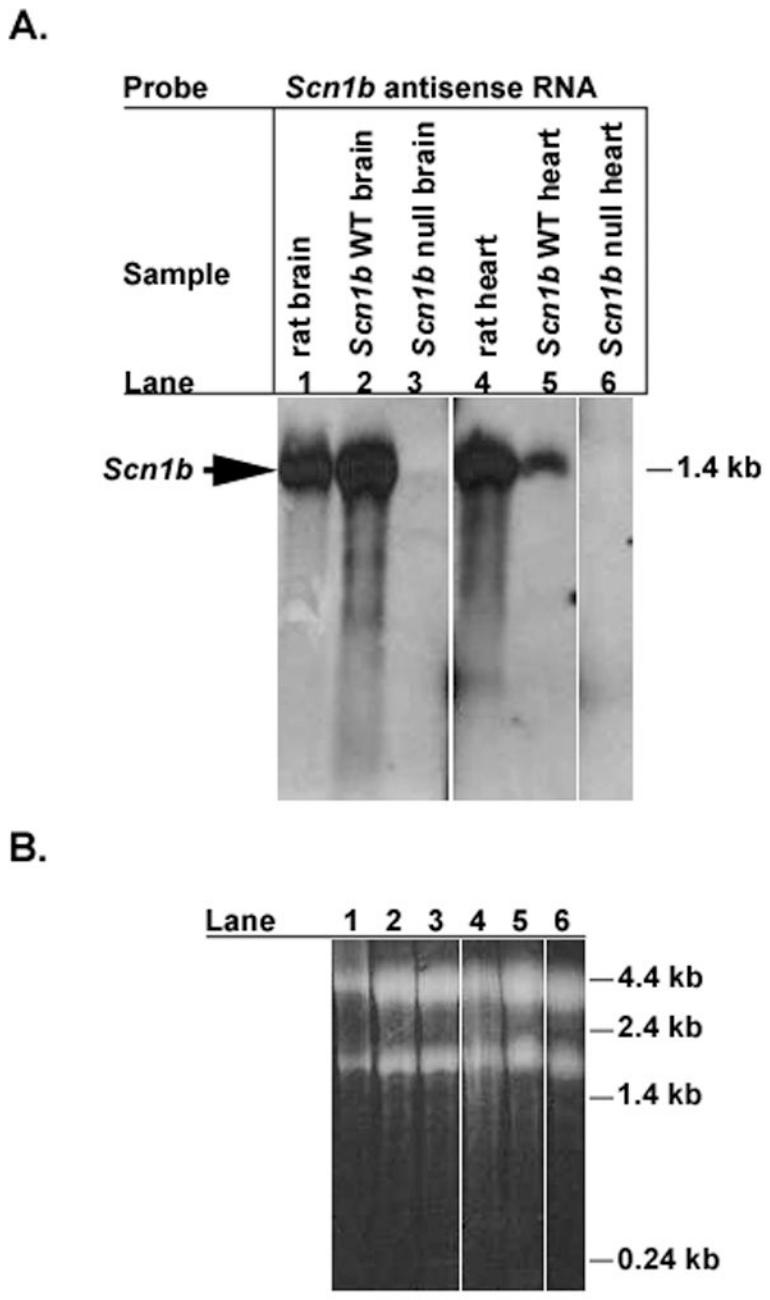

Fig. 1. Northern blot analysis of *Scn1b* null brain and heart

Total RNA was isolated from adult rat brain, adult rat heart, P17-18 *Scn1b* wildtype brain, P17-18 *Scn1b* wildtype heart, P17-18 *Scn1b* null brain, and P17-18 *Scn1b* null heart, as indicated in panel A. Equal aliquots of RNA (10 μg for brain samples, lanes 1–3; 20 μg for heart samples, lanes 4–6) were separated on agarose-formaldehyde gels and probed with a digoxigenin-labeled antisense *Scn1b* mRNA probe. A. Northern blot. Arrow indicates position of ~1.4 kilobase band corresponding to *Scn1b*. B. Ethidium bromide stained gel prior to transfer of RNA, showing approximately equal loading of RNA samples. 18S and 28S ribosomal RNAs are stained.

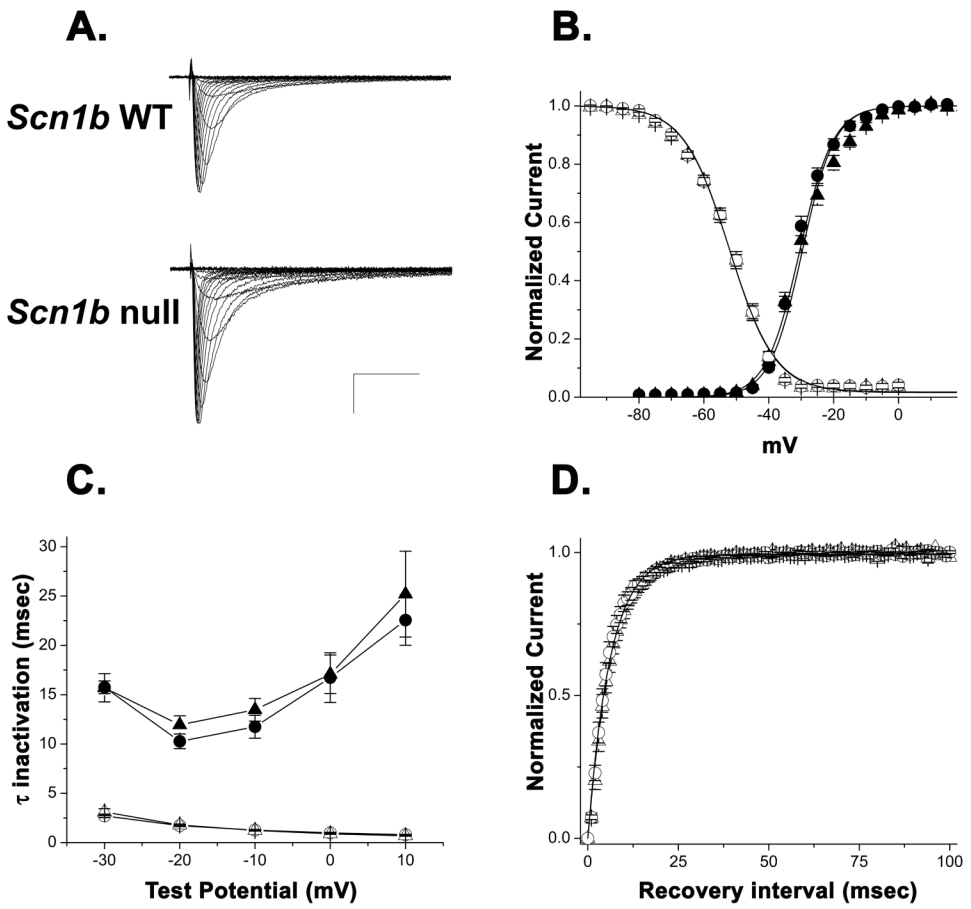

Fig. 2. Comparison of I_{Na} recorded from *Scn1b* wildtype and null ventricular myocytes

A. Representative I_{Na} densities recorded from*Scn1b* wildtype and null myocytes. Test pulses from −80 to +20 mV, with step of 5 mV. Scale bar: 15 pA/pF and 10 ms.

B. Mean activation (filled symbols) and inactivation (open symbols) curves for I_{Na} from *Scn1b* wildtype mice (circles; Activation: $V_{½}$ = −30.51 ± 0.6 mV, *k* = −5.17 ± 0.31 mV, n = 13 cells from 9 mice; Inactivation: $V_{½}$ = −52.14 ± 0.59, *k* = 7.07 ± 0.15, n = 12 cells from 9 mice) and *Scn1b* null mice (triangles; Activation: $V_{½}$ = −29.70 ± 1.0 mV, *k* = −5.00 ± 0.77 mV, n = 17 cells from 12 mice; Inactivation: $V_{½}$ = −52.12 ± 0.82, *k* = 7.02 ± 0.16, n = 15 cells from 11 mice). Smooth lines were generated by the Boltzmann equation using mean values for $V_{½}$ and *k* determined from fits of individual experiments.

C. Current inactivation kinetics as a function of voltage. Mean fast ($\tau_{fast,}$ open symbols) and slow (τ_{slow} closed symbols) time constants of inactivation.

D. Recovery from inactivation. Smooth lines represent a single exponential generated from the mean τ_{rec} values determined from fits of individual experiments. For *Scn1b* wildtype, τ_{rec} = 6.14 ± 0.57 ms, n = 8 cells from 5 mice. For *Scn1b* null τ_{rec} = 6.52 ± 0.60 ms, n = 5 cells from 5 mice. For B–D, data from *Scn1b* wildtype and null mice are represented by circles and triangles, respectively. Inactivation kinetics are summarized in Table 1. *p ≤ 0.05 from Student's t-test. For this and subsequent figures, error bars show SEM.

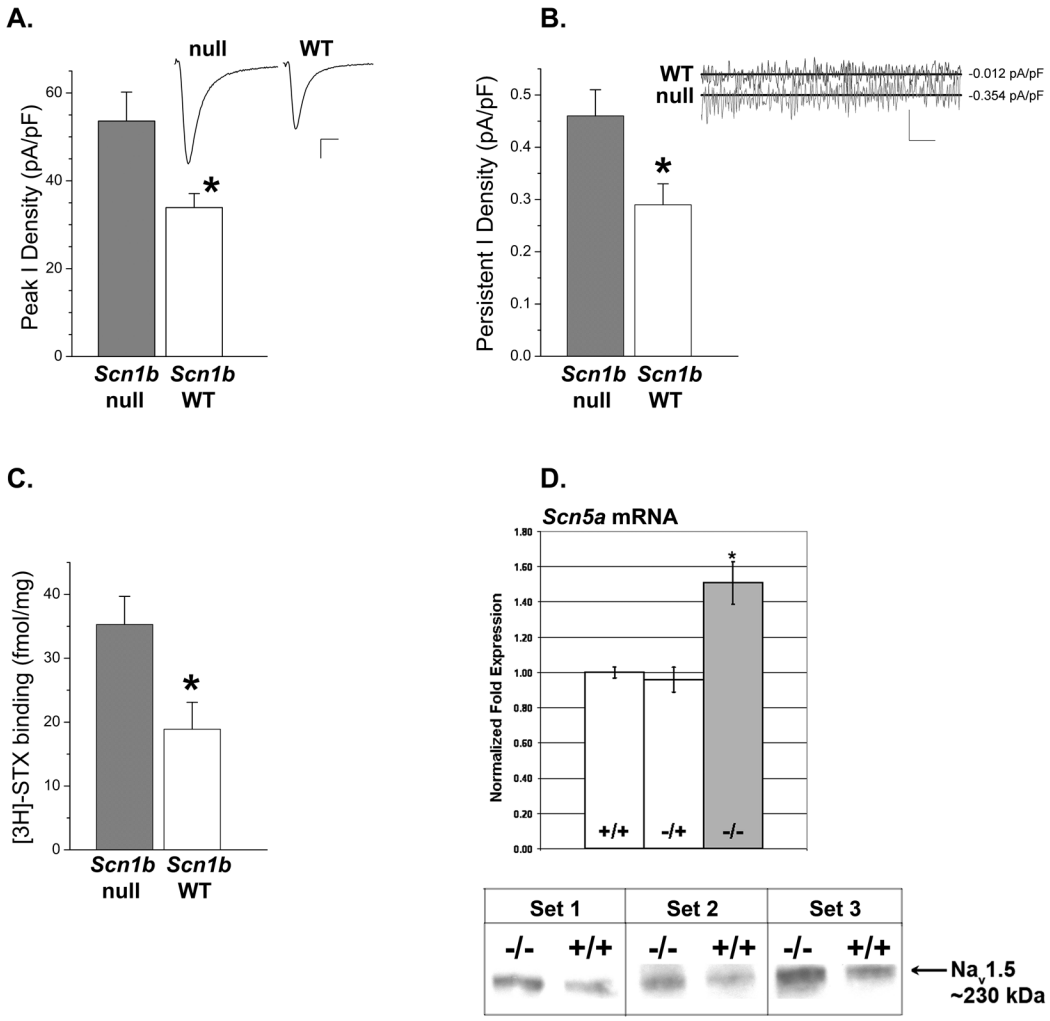

Fig. 3. Loss of β1 results in increased I_{Na} and I_{NaP} densities, increased ^{3}H-STX binding, and increased *Scn5a* expression

A. Average peak I_{Na} from ventricular myocytes. *Scn1b* wildtype (WT) = −33.9 ± 3.2 pA/pF; *Scn1b* null = −53.6 ± 6.6 pA/pF. *Inset for panel A*, typical I_{Na} traces (test pulse to −20 mV) corrected for cell capacitance recorded from *Scn1b* null myocytes (left) and *Scn1b* wildtype myocytes (right). Scale bar: 10 pA/pF and 2.5 ms.

B. I_{NaP} from ventricular myocytes. *Scn1b* wildtype = −0.29 ± 0.04 pA/pF; *Scn1b* null = −0.46 ± 0.05* pA/pF. Membrane capacitance: *Scn1b* wildtype = 74.2 ± 5.0 pF, *Scn1b* null = 52.9 ± 4.1* pF. For *Scn1b* wildtype n = 13 cells from 9 mice. For *Scn1b* null n = 17 cells from 12 mice. *Inset for panel B*, zoomed image of the traces shown in the inset to panel A, showing the current from 50–100 ms following the depolarizing pulse. Solid lines represent averaged amplitudes for this time segment, similar to the analysis performed in B. Scale bar: 0.5 pA/pF and 5 ms.

C. Specific [^{3}H]-STX binding (*Scn1b* wildtype: 18.9 ± 4.2 fmol/mg protein, n = 3; *Scn1b* null: 35.3 ± 4.4* fmol/mg protein, n = 3) in homogenized ventricular myocytes. *p ≤ 0.05 for *Scn1b* wildtype vs. *Scn1b* null.

D. Upper panel: *Scn5a* mRNA expression levels in *Scn1b* heterozygous (+/−, n = 6) and null (−/−, n = 7) heart tissue compared to wildtype (+/+) littermates (normalized to 1, n =7) using the ΔΔCt method to determine fold expression levels and Single Factor ANOVA to determine significance. *Scn5a* expression is 151% of wildtype in *Scn1b* null (*p = 0.002) and ~100% in

Scn1b heterozygous mice. Lower panel: Western blots of heart membranes prepared from 3 sets of *Scn1b* wildtype (+/+) and *Scn1b* null (−/−) littermate pairs showing an increase in $Na_V1.5$ protein in *Scn1b* null heart (133% of wildtype, $p = 0.03$). Each lane represents protein from one mouse.

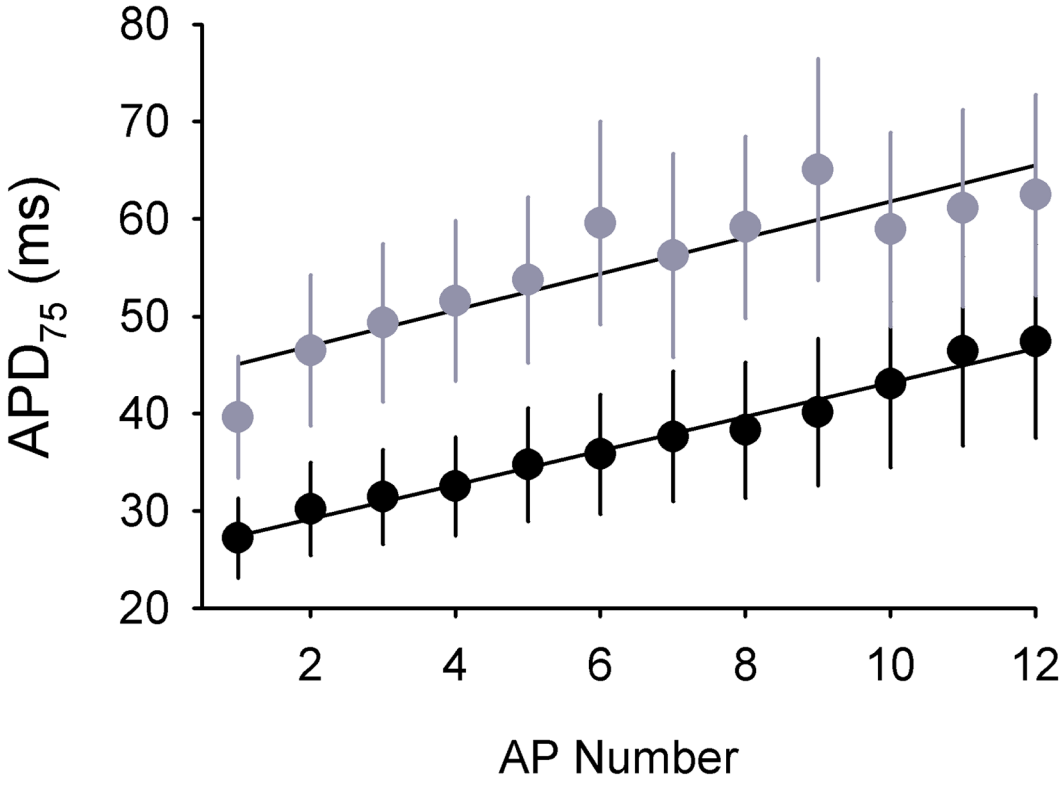

Fig. 4. Action potentials are prolonged in *Scn1b* null myocytes

APD_{75} values were measured in isolated *Scn1b* wildtype (n=14) and null (n=15) ventricular myocytes in response to stimulation at a cycle length of 150 ms. Solid lines are linear fits to the data. Analysis of the data using two-way ANOVA shows a significant ($p < 0.0001$) increase in APD_{75} in *Scn1b* null myocytes.

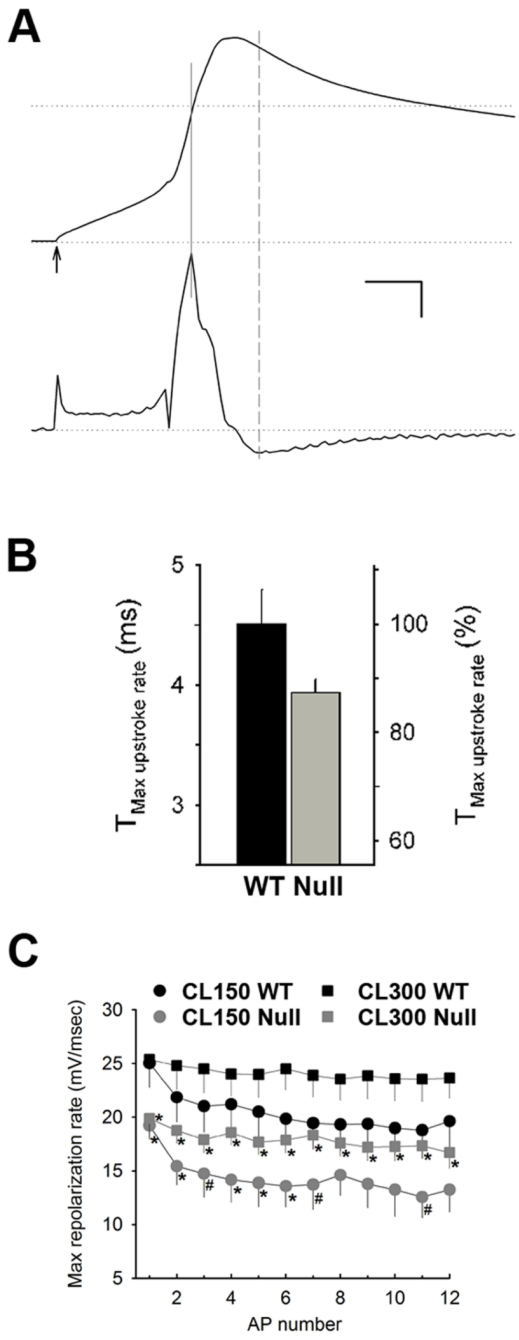

Fig. 5. Analysis of the rate of change in V_m for AP recordings

A. Details of an averaged trace of the first AP (150 ms CL), top panel; and the corresponding dV_m/dt, bottom panel. The arrow indicates the starting point of the stimulation pulse. Vertical solid line indicates the maximal depolarizing rate and dotted line indicates the maximal repolarizing rate. Scale bars: 1.5 ms and 20 mV/ms.

B. Maximum upstroke rate for the first action potential in each train for CL150 recorded from *Scn1b* wildtype (WT, black) or *Scn1b* null (Null, gray) myocytes. Analysis of the data using two-way ANOVA shows a significant (p=0.0021) decrease for *Scn1b* null myocytes.

C. Maximum repolarization rate recorded from *Scn1b* wildtype (WT, black) or *Scn1b* null (Null, gray) myocytes for CL150 (circles) or CL300 (squares). *$p < 0.05$ or $^{\#}p < 0.10$ for *Scn1b* wildtype vs. *Scn1b* null mice.

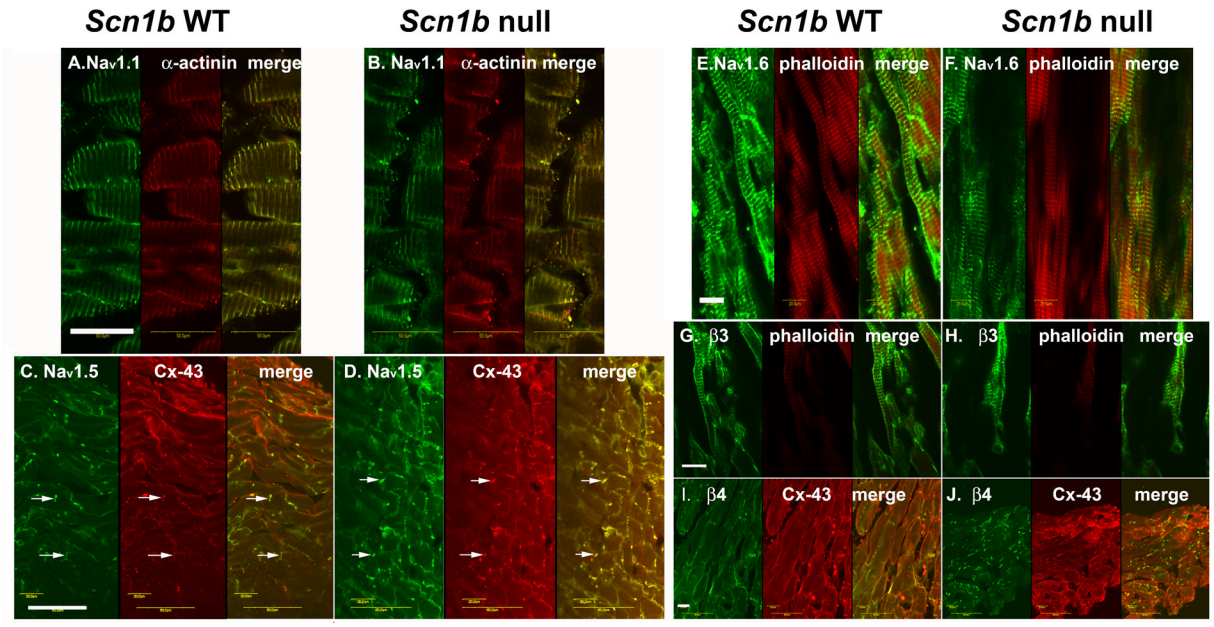

Fig. 6. Loss of β1 does not affect the localization of sodium channels or structural proteins

A, **C**, **E**, **G, and I** sections from *Scn1b* wildtype hearts. **B**, **D**, **F**, **H, and J** sections from *Scn1b* null hearts.

A and **B**, $Na_v1.1$ (green) co-localizes with α-actinin (red) at the Z-line/t-tubules in heart sections. Scale bar 50 μm.

C and **D**, co-localization of $Na_v1.5$ (green) with connexin-43 (Cx-43) (red) at intercalated disks (examples are shown at arrows). Scale bar 50 μm.

E and **F**, $Na_v1.6$ (green) and phalloidin (red) co-localize at Z-line/t-tubules. Scale bar 20 μm.

G and **H**, co-localization of β3 (green) and phalloidin (red). Scale bar 20 μm.

I and **J**, β4 (green) co-localizes with connexin-43 (Cx-43) (red). Scale bar 20 μm.

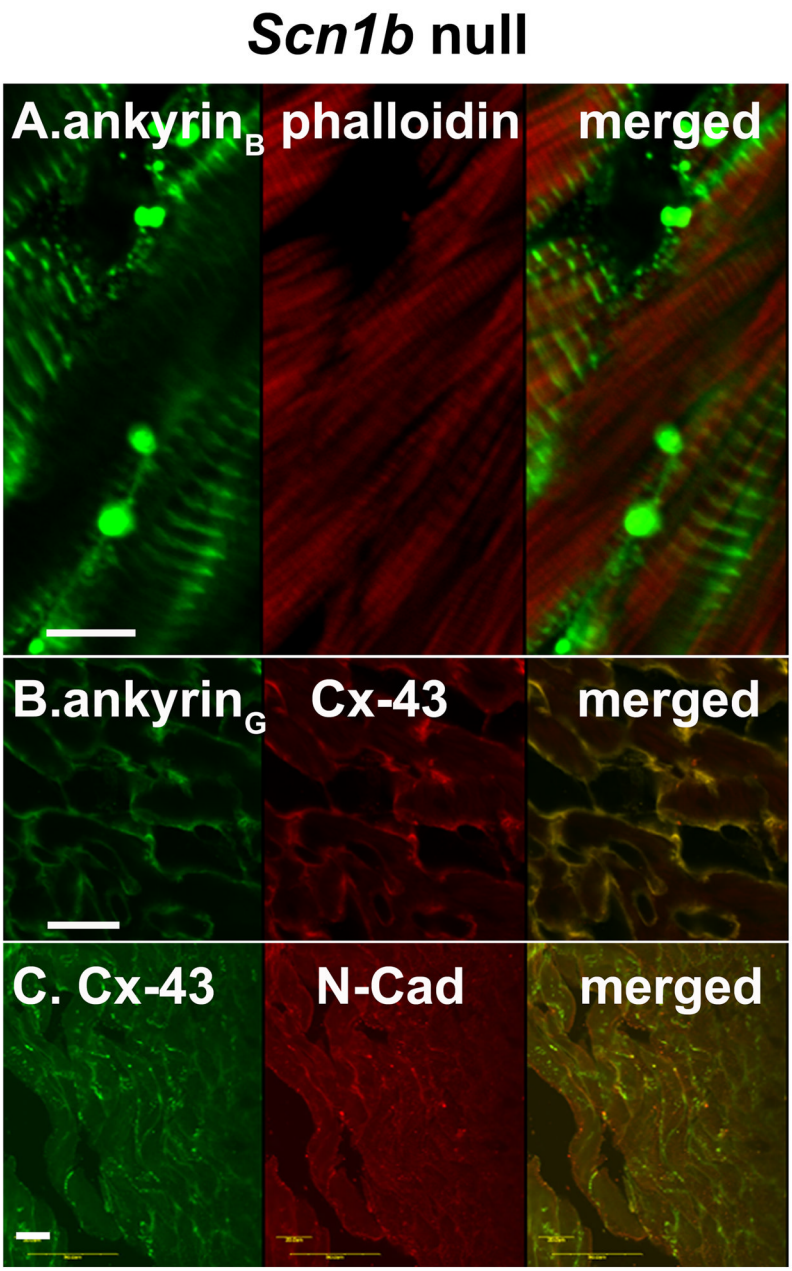

Fig. 7. Localization of ankyrin$_B$, ankyrin$_G$, connexin-43, and N-cadherin in *Scn1b* null cardiac myocytes

A. Co-localization of ankyrin$_B$ (green) with phalloidin (red). Scale bar 100 μm.

B. Co-localization of ankyrin$_G$ (green) with connexin-43 (Cx-43) (red). Scale bar 20 μm.

C. Co-localization of connexin-43 (Cx-43, green) with N-cadherin (red). Scale bar 20 μm.

Table 1

I_{Na} inactivation kinetics in myocytes as a function of voltage.

***Scn1b* null, n= 15 (12)**					***Scn1b* wildtype, n= 12 (9)**			
$\tau_{slow\ (ms)}$	**$\tau_{fast\ (ms)}$**	**A^1**	**A^2**	**V-test $_{(mV)}$**	**$\tau_{slow\ (ms)}$**	**$\tau_{fast\ (ms)}$**	**A^1**	**A^2**
25.2±4.3	0.7±0.04*	0.04±0.01	0.96±0.01	+10	22.6±2.6	0.8±0.04	0.04±0.01	0.96±0.01
17.1±2.0	0.9±0.05	0.04±0.01	0.96±0.01	+0	16.7±2.5	1.0±0.05	0.05±0.01	0.95±0.01
13.5±1.2	1.2±0.06	0.06±0.01	0.94±0.01	−10	11.7±1.2	1.3±0.07	0.08±0.01	0.92±0.01
11.9±0.9	1.8±0.10	0.12±0.01	0.88±0.01	−20	10.2±0.7	1.7±0.1	0.12±0.01	0.88±0.01
15.7±1.4	3.1±0.34	0.17±0.01	0.83±0.01	−30	15.7±0.6	2.7±0.18	0.15±0.01	0.85±0.01

τ_{fast} and τ_{slow} represent the fast and slow components of the current inactivation time-course, respectively (Fig. 1C); A^1 and A^2 represent their relative amplitudes as measured at different test potentials (V-test).

*$p \leq 0.05$.

Table 2

ECG characteristics of *Scn1b* wildtype, null, and heterozygous mice.

CONTROL									
	n	**P duration (ms)**	**QRS (ms)**	**PR (ms)**	**QTPeak (ms)**	**QT90 (ms)**	**RR (ms)**	**R-amp (mV)**	**QT_{90C} (ms)**
WT	27	10.61±0.33	8.62± 0.32	46.60±1.58	17.41±0.61	27.23±0.96	162.1±5.5	1.49±0.07	19.3±0.07
Null	29	10.39±0.32	8.98± 0.29	49.18±1.57†	20.87±0.58*	32.42±0.99*	181.8±5.7*	1.46±0.07	33.12±0.10
Het	48	10.00±0.32	8.67± 0.22	46.22±0.96	17.66±0.41	27.57±0.63	163.3±3.2	1.58±0.05	22.2±0.08
PROPRANOLOL & ATROPINE									
	n	P duration (ms)	QRS (ms)	PR (ms)	QT_{Peak} (ms)	QT_{90} (ms)	RR (ms)	R-amp (mV)	QT_{90C} (ms)
WT	8	11.81±0.5§	10.20±0.8$^{¢}$	48.51±2. 5	20.24±1.3$^{¢}$	28.66±1.3	174.2±6.8	1.37±0.07	16.61±0.1
Null	10	11.34±0.6$^{¢}$	9.58±0.5$^{¢}$	47.57±1.4	23.91±0.9$^{¢*}$	35.41±1.0*	205.5±4.7§*	1.30±0.08	43.82±0.3
Het	13	11.64±0.3§	10.74±0.6$^{¢}$	45.94±1.5	20.38±0.6$^{¢}$	28.92±0.9	171.9±7.4	1.33±0.08	23.34±0.1

ECG data are tabulated before (control) and after autonomic block. P represents the duration of the P wave, while QT_{PEAK} represents the interval from the onset of the Q wave to the peak of the T wave. QT_{90} is the time duration from Q to 90% decay of the T wave from peak to baseline. QT_{90C} represents the QT_{90} duration corrected for heart rate [24]. R-amp denotes the amplitude of the R wave. Data were analyzed as described in *Methods (Investigator 1)*.

* $p \leq 0.05$ for *Scn1b* null (Null) vs. both *Scn1b* wildtype (WT) and *Scn1b* heterozygous (Het) mice, with $p > 0.1$ for WT vs. Het.

† $p \leq 0.1$ for Null vs. Het only, with $p > 0.1$ for both Null vs. WT, and WT vs. Het.

$^{¢}$ $p \leq 0.05$

§ $p \leq 0.1$ for control vs. propranolol and atropine recordings.

Similar results (not shown) were observed using an alternative analysis protocol (*Methods, Investigator 2)*, which also included measurements of (control) heart rate corrected Q to end of T interval (QT_{100c})*; Scn1b* wildtype = 50.40 ± 0.17 ms n = 26, *Scn1b* null =79.04 ± 0.19 ms n = 30, *Scn1b* heterozygous = 44.93 ± 0.23 ms n = 41.